Investigation the BER Characteristics of Hexagonal Multicarrier Modulation in the Presence of System Impairments

A. H. Majeed
Department of Laser and Optoelectronics Engineering, College of Engineering, Al-Nahrain University, Baghdad, Iraq
Email:asmaahameed37@yahoo.co.uk

Abstract —Hexagonal Multicarrier Modulation (HMM) is based on arranging the information data in a hexagonal manner in the time-frequency plane to mitigate interference in a doubly dispersive wireless channel. This paper investigates the bit error rate characteristics of this modulation scheme theoretically in the presence of timing offset and carrier frequency offset. The simulation results show clearly that the HMM system can tolerate more offset compared with a conventional OFDM counterpart.

Index Terms—TF lattice, HMM lattice, OFDM modulation, BER

I. Introduction

Wireless communication systems usually use Orthogonal Frequency-Division Multiplexing (OFDM) modulation to overcome performance degradation due to fading channel [1], [2]. The OFDM scheme is a multicarrier modulation (MCM) in which the high bit rate stream is split into several low bit rate substreams and transmitted, in parallel, on several subcarriers. Recently, there is an increasing interest in a Doubly Dispersive (DD) wireless channel that is time dispersive and frequency dispersive [3], [4]. The channel is selective in time as well as in frequency. The channel frequency selectivity arises from the intersymbol interference as a result of the multipath propagation, while the channel time selectivity arises from the Doppler shift and/or the carrier frequency offset between the transmitter and receiver. This channel spreads the OFDM signal simultaneously in both frequency and time domains. Due to this spreading, the DD channel introduces both intercarrier interference (ICI) and intersymbol interference (ISI) which degrade the system performance [5], [6]. The OFDM scheme, supported with zero padding or cyclic prefix guard time interval, can combat ISI efficiently.

Conventional OFDM systems are based on rectangular type pulses and therefore they can not combat ICI [7]. Several pulse-shaping OFDM systems have been proposed in the literature which uses rectangular Time-Frequency (TF) lattices to yield suboptimal transmission in DD channels [8]-[10]. Recently, Han and Zhang [11] have proposed a Hexagonal Multicarrier Modulation (HMM) scheme in which they considered the signal transmission as based on a hexagonal TF lattice. The pulse shape of the modulation waveform and the lattice parameters are optimized jointly to adapt to the channel scattering function in order to optimally combat the impact of the propagation channel. The effects of insufficient synchronization on the phase and amplitude of the demodulated symbol by using a projection receiver in HMM systems have been addressed theoretically by Xu and Shen [12]. The authors in this reference have also discussed the effects of Carrier Frequency Offset (CFO), Timing Offset (TO), and the spread factor of the channel on the performance of signal-to–interference–plus-noise ratio (SINR) in HMM modulation systems. Further, Hand and Zhang [13] have proposed a parallel maximum–like hood sequence detection scheme for HMM with time-frequency localized pulses to enhance the system performance.

This paper aims to address the Bit Error Rate (BER) characteristics of HMM systems in the presence of various system impairments such as timing offset, carrier frequency offset, and channel spread factor. The results are compared with those related to a conventional OFDM system to show the robustness of HMM as a transmission scheme in the doubly dispersive channel.

II. Theory

The transmission of multiplexed signals can be described using the concept of TF lattice. For example, the conventional Time-Division Multiplexed (TDM) signal can be considered as transmitting one-dimensional lattice along the time axis

$$\mathrm{V}_{TDM} = \begin{bmatrix} T \\ 0 \end{bmatrix} \tag{1}$$

where T denotes the time slot for each sub-channel.

The conventional frequency division multiplexed (FDM) signal can be viewed as the transmission on one-dimensional lattice along the frequency axis

$$\mathrm{V}_{FDM} = \begin{bmatrix} F \\ 0 \end{bmatrix} \tag{2}$$

where F stands for subcarrier frequency separation. The conventional OFDM signal creates a two-dimensional rectangular lattice [12]

Manuscript received November 2, 2018; revised June 3, 2019.
doi:10.12720/jcm.14.7.566-573

$$V_{OFDM} = \begin{bmatrix} T & 0 \\ 0 & F \end{bmatrix} \tag{3}$$

where T and F denote respectively, symbol period and subcarrier separation.

In HMM signaling, pulses bearing the information are organized in a hexagonal lattice and can be adequately separated in the TF plane. Fig. 1 shows an example of the hexagonal transmission pattern which is described by [11]

$$V_{HMM} = \begin{bmatrix} T/2 & 0 \\ F/2 & F \end{bmatrix} \tag{4}$$

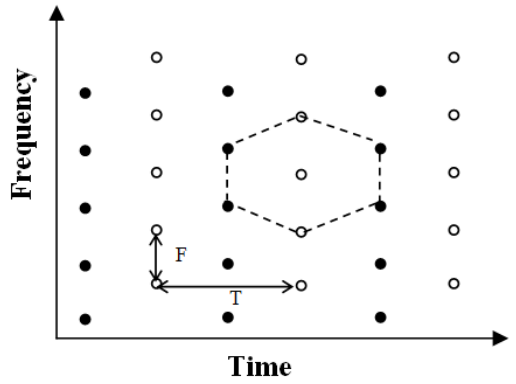

Fig. 1. Partition of the hexagonal lattice into a rectangular sub lattice $\mathbf{V}_{RECT1}$ (denoted by ●) and its coset $\mathbf{V}_{RECT2}$ (denoted by ○) [12].

The transmitted signal can be expressed as

$$s(t) = \sum_m \sum_n c_{mn} g_{mn}(t) \tag{5a}$$

where

$$g_{mn}(t) = g(t - m\frac{T}{2}) e^{j2\pi(m+2n)(F/2)t} \tag{5b}$$

Here c_{mn} is the data symbol which is usually taken from a specific signal constellation and g(t) is the Gaussian pulse

$$g(t) = (\frac{2}{\sigma^2})^{1/4} e^{-\pi(t/\sigma)^2} \tag{6}$$

In eqn. 6, σ^2 stands for the time width of the pulse and determines the energy distribution of the pulse in the time and frequency directions.

The original hexagonal lattice depicted in Fig. 1 can be viewed as the disjoint union of two rectangular sublattices, $\mathbf{V}_{RECT1}$ and $\mathbf{V}_{RECT2}$, where symbols are denoted by a_{mn} and b_{mn} [12]

$$s(t) = \sum_m \sum_n a_{mn} A_{mn}(t) + b_{mn} B_{mn}(t) \tag{7a}$$

$$A_{mn}(t) = g(t - mT) e^{j2\pi mFt} \tag{7b}$$

$$B_{mn}(t) = g(t - (m + \frac{1}{2})T) e^{j2\pi(n+1/2)Ft} \tag{7c}$$

After transmission along DD channel, the received signal can be expressed as

$$r(t) = h(t, \tau) * s(t) + n(t) \tag{8}$$

where h(t,τ) is the time-varying impulse response of the channel, n(t) is the additive white Gaussian noise (AWGN), and * denotes convolution. The first term in eqn. 8 can be expressed as

$$h(t,\tau) * s(t) = \int_0^{\tau_{\max}} \int_{-f_d}^{f_d} H(\nu,\tau) s(t-\tau) e^{j2\pi\nu t} d\tau d\nu \tag{9}$$

where

H (ν,τ) = Delay–Doppler spread function
= Fourier transform of h (t,τ) with respect to "t"

f_d = Maximum Doppler frequency

τ_{max} = Maximum multipath delay spread.

The analysis in Ref. [12] shows that if a DD channel with exponential delay power profile and U-shape Doppler power spectrum is considered, the projection receiver gives the following expressions for the signal energy $E_S(\Delta t, \Delta f, \tau_{rms}, f_d)$ and interference–plus-noise energy $E_{IN}(\Delta t, \Delta f, \tau_{rms}, f_d)$

$$E_S(\Delta t, \Delta f, \tau_{rms}, f_d) = \frac{\sigma_c^2}{\pi \tau_{rms} f_d} \int_0^{\infty} e^{-\tau/\tau_{rms}} e^{-(\pi/\sigma^2)(\tau-\Delta t)^2} d\tau \int_{-f_d}^{f_d} \frac{e^{-\sigma^2\pi(\nu+\Delta f)^2}}{\sqrt{1-(\nu/f_d)^2}} d\nu \tag{10}$$

$$E_{IN}(\Delta t, \Delta f, \tau_{rms}, f_d) = \frac{\sigma_c^2}{\pi \tau_{rms} f_d} \left\{ \sum_{(m,n)\neq(0,0)} \int_0^{\infty} e^{-\tau/\tau_{rms}} e^{-\pi(mT+\tau-\Delta t)^2/\sigma^2} d\tau \times \int_{-fd}^{fd} \frac{e^{-\sigma^2\pi(nF+\nu+\Delta f)^2}}{\sqrt{1-(\nu/f_d)^2}} d\nu \right.$$
$$\left. + \sum_{(m,n)\neq(0,0)} \int_0^{\infty} e^{-\tau/\tau_{rms}} e^{-\pi((m+1/2)T+\tau-\Delta t)^2/\sigma^2} d\tau \times \int_{-fd}^{fd} \frac{e^{-\sigma^2\pi((n+1/2)F+\nu+\Delta f)^2}}{\sqrt{1-(\nu/f_d)^2}} d\nu \right\}$$
$$+ \sigma_n^2 |Q_p(0,0)| \tag{11}$$

where

σ_c^2 = Average power of the data symbols

Δt = Timing offset

Δf = Carrier frequency offset

τ_{rms} = r.m.s delay spread

σ_n^2 = Variance of the AWGN

In eqn. 11, $|Q_p(0,0)|$ denotes $|Q_p(\tau,\nu)|$, when τ=ν=0 . Further, Q_p represents the ambiguity function corresponding to the used–shape pulse p (t)

$$Q(\tau,\nu) = \int_{-\infty}^{\infty} p(t) \cdot p^*(t-\tau) e^{-j2\pi\nu t} dt \tag{12a}$$

where the superscript * denotes the complex conjugate. For the Gaussian pulse defined in eqn. 6, the ambiguity function reads

$$Q(\tau,\nu) = \int_{-\infty}^{\infty} g(t) \cdot g^*(t-\tau) e^{-j2\pi\nu t} dt$$
$$= e^{-(\pi/2)((1/\sigma^2)\tau^2 + \sigma^2\nu^2)} e^{-j\pi\tau\nu} \tag{12b}$$

Therefore, $\left|Q_g(0,0)\right| = 1$.

Investigating Eqns. 10 and 11 reveal the following findings:

- Both signal energy and interference–plus-noise energy are a function of carrier frequency offset, timing offset, and channel spread factor $\tau_{rms}f_d$.
- In the absence of CFO and TO, the channel spread factor $\tau_{rms}f_d$ plays a key role in determining system performance. The signal energy E_{S0} and interference energy E_{I0} are then given, respectively, by

$$E_{S0}(\tau_{rms}, f_d) = \frac{\sigma_c^2}{\pi\tau_{rms}f_d}\int_0^{\infty} e^{-\tau/\tau_{rms}} e^{-(\pi/\sigma)\tau^2} d\tau \int_{-f_d}^{f_d} \frac{e^{-\sigma\pi v^2}}{\sqrt{1-(v/f_d)^2}} dv, \quad (13a)$$

$$E_{IN0}(\tau rms, f_d) = \frac{\sigma_c^2}{\pi\tau_{rms}f_d}\left\{\sum_{(m,n)\neq(0,0)}\int_0^{\infty} e^{-\tau/\tau_{rms}} e^{-\pi(mT+\tau)^2/\sigma^2} d\tau \times \int_{-f_d}^{f_d} \frac{e^{-\sigma^2\pi(nF+v)^2}}{\sqrt{1-(v/f_d)^2}} dv \right.$$

$$\left. + \sum_{(m,n)\neq(0,0)}\int_0^{\infty} e^{-\tau/\tau_{rms}} e^{-\pi((m+1/2)T+\tau)^2/\sigma^2} d\tau \times \int_{-f_d}^{f_d} \frac{e^{-\sigma^2\pi((n+1/2)F+v)^2}}{\sqrt{1-(v/f_d)^2}} dv \right\}$$

$$SIN = \left(\int_0^{\infty} e^{-\tau/\tau rms} e^{-(\pi/\sigma^2)(\tau-\Delta t)^2} \int_{-fd}^{f_d} \frac{e^{-\sigma^2\pi(nF+v+\Delta f)^2}}{\sqrt{1-(v/f_d)^2}} dv \right) \times \left(\sum(m,n)\neq(0,0) \int_0^{\infty} e^{-\tau/\tau_{rms}} e^{-\pi(mT+\tau-\Delta t)^2/\sigma^2} d\tau \right.$$

$$\left. \times \int_{-fd}^{f_d} \frac{e^{-\sigma^2\pi(nF+v+\Delta f)^2}}{\sqrt{1-(v/f_d)^2}} dv + \sum(m,n)\neq(0,0) \int_0^{\infty} e^{-\tau/\tau_{rms}} e^{-\pi((m+1/2)T+\tau-\Delta t)^2/\sigma^2} d\tau \times \int_{-fd}^{f_d} \frac{e^{-\sigma^2\pi(nF+v+\Delta f)^2}}{\sqrt{1-(v/f_d)^2}} dv \right)^{-1} \quad (16)$$

III. Numerical and Simulation Results

This section is devoted to present numerical results to characterize the SIR of a HMM system operating with non-ideal transmission conditions. Further, the corresponding BER characteristics are reported by simulating the system in MATLAB environment. Results related to a conventional OFDM system here for comparison purposes. Unless otherwise stated, the parameters values used in the numerical and simulation results are listed in Table I. Simulation results are obtained by sending 1Mbit-block of data.

We follow the same scenario adopted in Refs. [11], [12] to set the frame for producing the results

- The parameter σ of the Gaussian pulse is chosen to be equal to $[T/\sqrt{3F}]^{1/2}$ to ensure optimum system parameters for a DD channel with exponential–U scattering function. For T=100μs and Δf =31.25 KHz, σ ≈43 μs.
- The results are presented for different values of the three parameters, carrier frequency offset Δf, timing offset Δt, and channel spread factor $\tau_{rms}f_d$. It is assumed that τ_{rms}/fd of the DD channel is fixed which ensures a fixed hexagonal transmission pattern. Obviously, when the channel spread factor increases, both τ_{rms} and f_d increase simultaneously.

$$+\sigma_n^2\left|Q_p(0,0)\right| \quad (13b)$$

- From the energy point of view, the interference and AWGN appear as independent parameters

$$E_{IN} = E_I + E_N \quad (14a)$$

where the noise energy

$$E_N = \sigma_n^2\left|Q_p(0,0)\right| = \sigma_n^2 \quad (14b)$$

Therefore, the signal–to–noise ratio SNR can be expressed as

$$SNR = \frac{\sigma_c^2}{\pi\sigma_n^2\left|Q_p(0,0)\right|\tau_{rms}f_d}\int_0^{\infty} e^{-\tau/\tau_{rms}} e^{-(\pi/\sigma^2)(\tau-\Delta t)^2} d\tau \int_{-f_d}^{f_d} \frac{e^{-\sigma^2\pi(v+\Delta f)^2}}{\sqrt{1-(v/f_d)^2}} dv \quad (15)$$

Further, the signal-to-interference ratio (SIR) is expressed as

- In all the numerical and simulation results, Δt and Δf are respectively normalized to T/2 and F/2.

TABLE I: PARAMETERS VALUES USED IN THE SIMULATION

Parameter	Values
Center carrier frequency	5GHz
Number of subcarriers	64
Sampling interval	1μs
Symbol period	100μs
Subcarrier frequency separation	31.25KHz
Modulation	QPSK
Cyclic prefix guard interval	26
Coding	RS(15,11)

Fig. 2 shows a simplified block diagram for the system under investigation. The transmitter uses Reed-Solomon encoder, RS(15,11), as a forward error correcting code. Further, a pilot – assisted channel estimation is adopted in the system.

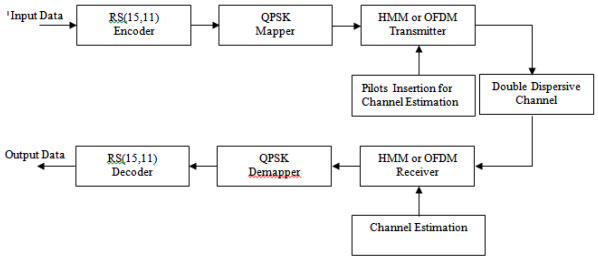

Fig. 2. System block diagram

Figs. 3a and 3b show, respectively, the received eye diagrams and signal constellations when the channel estimation scheme is OFF and ON. The results are reported for both HMM and OFDM systems when SNR=30dB, $\tau_{rms}f_d$ =0.02, and $\Delta t=\Delta f=0$. The effect of carrier frequency offset $\Delta f= \pm 0.2$ with $\Delta t=0$ are taken into account in Fig. 4. Fig. 5 shows the effect of $\Delta t =0.2$ on the system performance when $\Delta f=0$ and the simulation is repeated in Fig. 6 when $\Delta t=-0.2$. The results in Figs. 3-6 highlight the following finding. The HMM system gives better performance than the OFDM counterpart, even in the absence of offset (i.e, $\Delta t=\Delta f=0$), and this conclusion is more pronounced in the presence of CFO and TO.

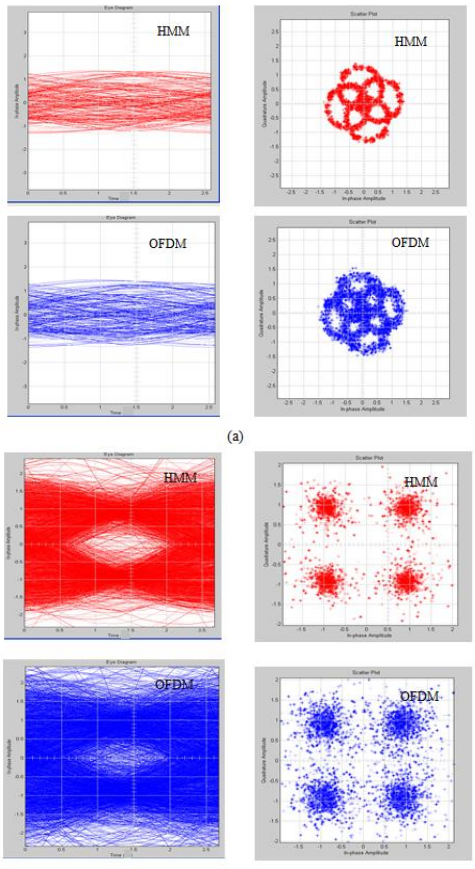

Fig. 3. Received eye diagrams and signal constellations when SNR =30dB, $\tau_{rms}f_d$ =0.02, and $\Delta t=\Delta f=0$ (a) Without channel estimation (b) with channel estimation.

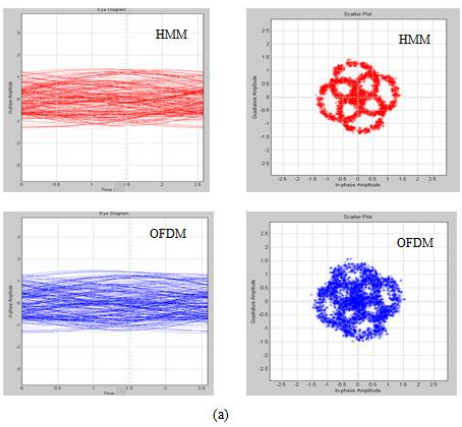

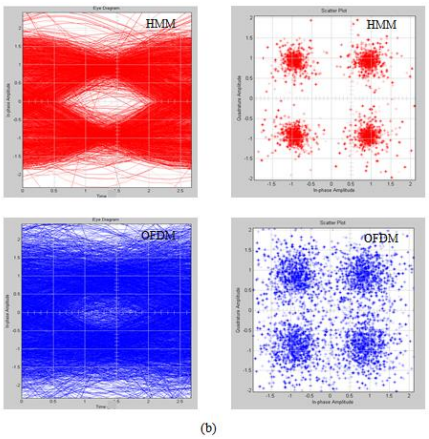

Fig. 4. Received eye diagrams and signal constellations when SNR =30dB, $\tau_{rms}f_d$ =0.02, and $\Delta t=0$, $\Delta f=\pm 0.2$ (a) Without channel estimation (b) with channel estimation.

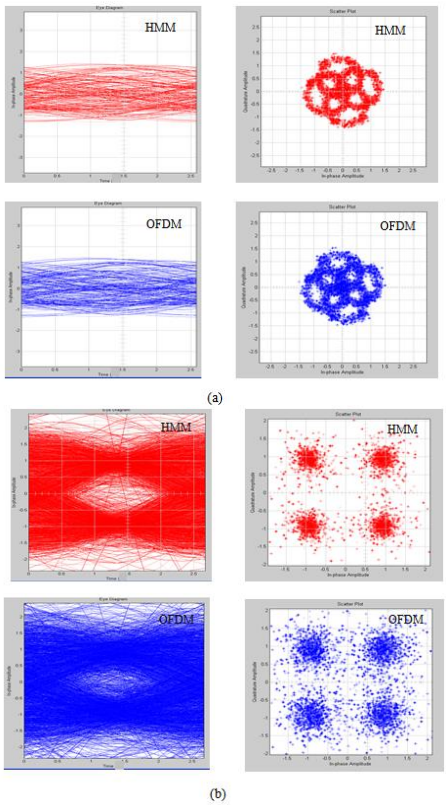

Fig. 5. Received eye diagrams and signal constellations when SNR =30dB, $\tau_{rms}f_d$ =0.02, and $\Delta f=0$, $\Delta t=+0.2$ (a) Without channel estimation (b) with channel estimation.

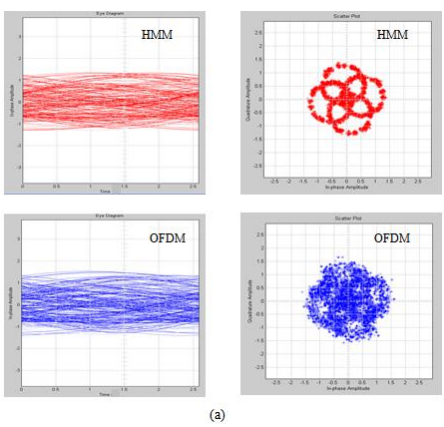

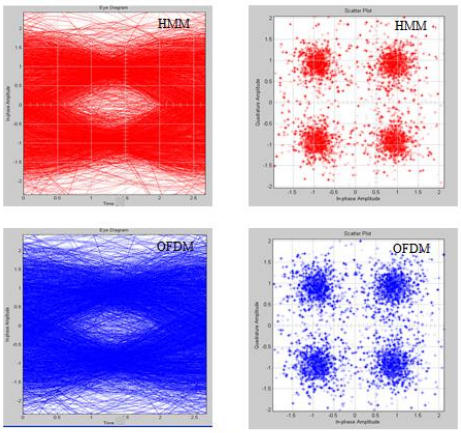

(b)

Fig. 6. Received eye diagrams and signal constellations when SNR =30dB, $\tau_{rms}f_d$ =0.02, and Δf=0, Δt=-0.2.(a) Without channel estimation (b) with channel estimation.

Figs. 7a-c show the effect of TO on signal-to-interference ratio (SIR) for SNR=10dB, 20dB and 30dB, respectively. The results are presented for three values of channel spread factor, $\tau_{rms}f_d$ =0.005, 0.01 and 0.02, when CFO is zero. Note that at SNR=10dB and Δt=Δf=0, the SIR of the HMM (OFDM) system are 18.3 (15.87), 15.87 (13.04), and 13.85dB (10.02dB) when $\tau_{rms}f_d$ =0.005, 0.01 and 0.02, respectively. These values are to be compared with 19.52 (16.7), 18.28 (13.6), and 16.7dB (10.29dB) when SNR increases to 30dB. In the presence of 10% TO, the corresponding SIR are 19.13 (9.53), 18.7 (9.25), and 15.4dB (8.2dB) when SNR=10dB and 20.45 (10.04), 19.47 (10.04) and 17.87dB (9.03dB) when SNR=30dB. Investigating these results highlights that the HMM system offers higher SIR compared with a conventional OFDM system even in the presence of TO.

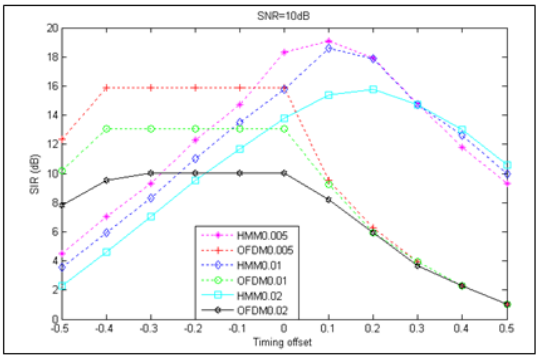

(a)

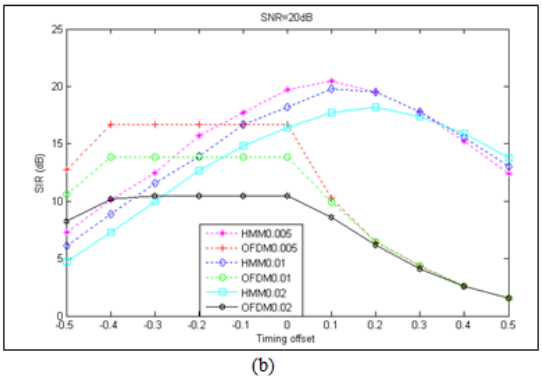

(b)

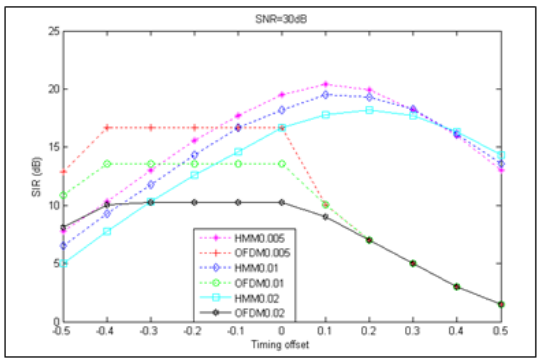

(c)

Fig. 7. Effect of Timing offset on signal-to-interference ratio (SIR) (a) SNR=10dB, (b) 20dB and (c) 30dB.

The calculations in Fig. 7 are repeated to address the effect of CFO on SIR when TO = 0 and the results are displayed in Fig. 8. Again the results highlight the robustness of the HMM system against the carrier frequency offset.

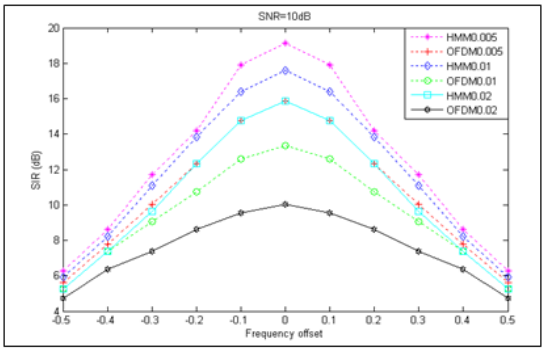

(a)

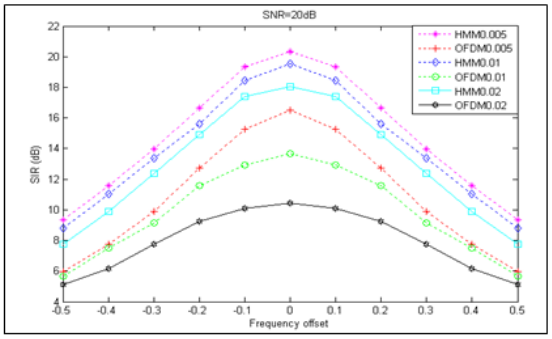

(b)

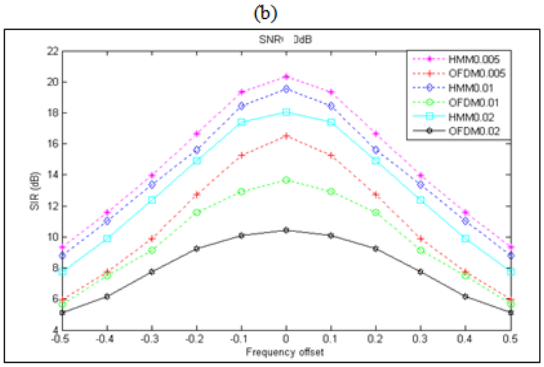

(c)

Fig. 8. Effect of carrier frequency offset on SIR when TO = 0 (a) SNR=10dB, (b) 20dB and (c) 30dB,

Figs. 9a and 9b show, respectively, the effect of TO on the BER characteristics of the HMM and OFDM systems operating without and with RS encoding. The simulation repeated in Figs. 10a and 10b to assess the effect of CFO on the BER characteristics in the absence and presence of coding, respectively. The BER performance of the two systems in the absence of TO and CFO is estimated from Figs. 8 and 9 and the results are listed in Table II for different values of SNR and channel spread factor.

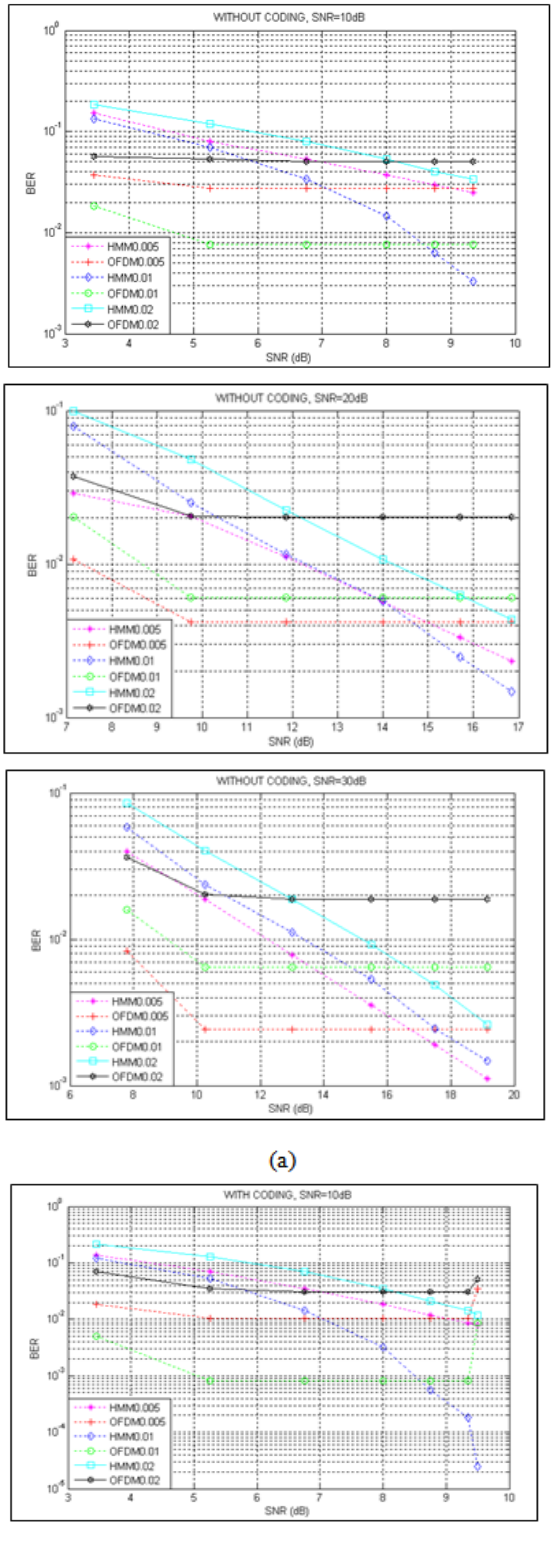

(a)

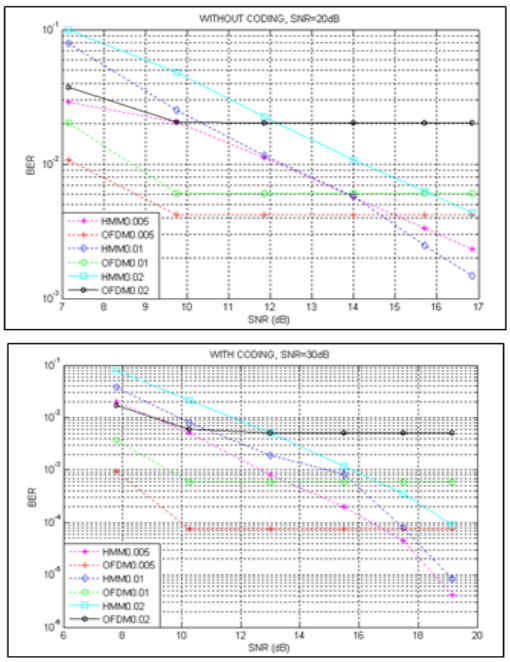

(b)

Fig. 9. Effect of TO on the BER characteristics of the HMM and OFDM systems (a) without coding (b) with coding.

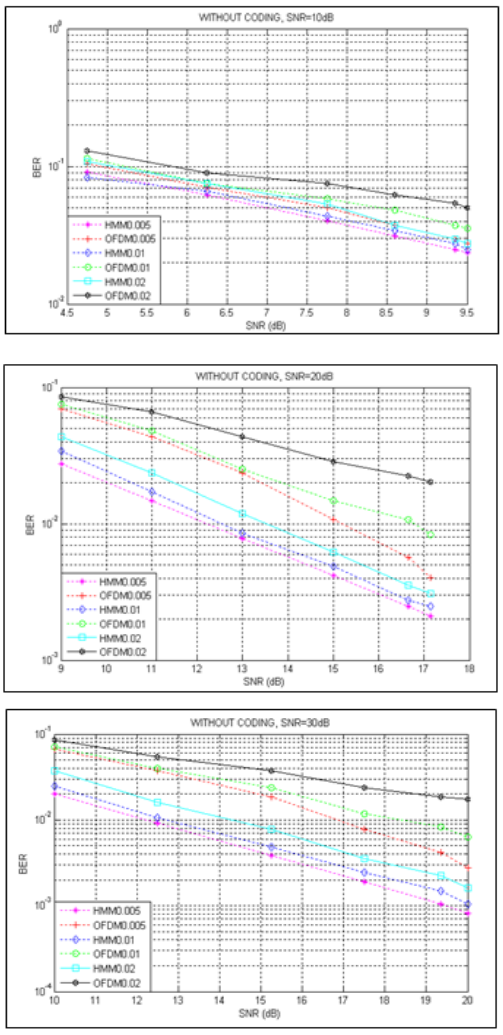

(a)

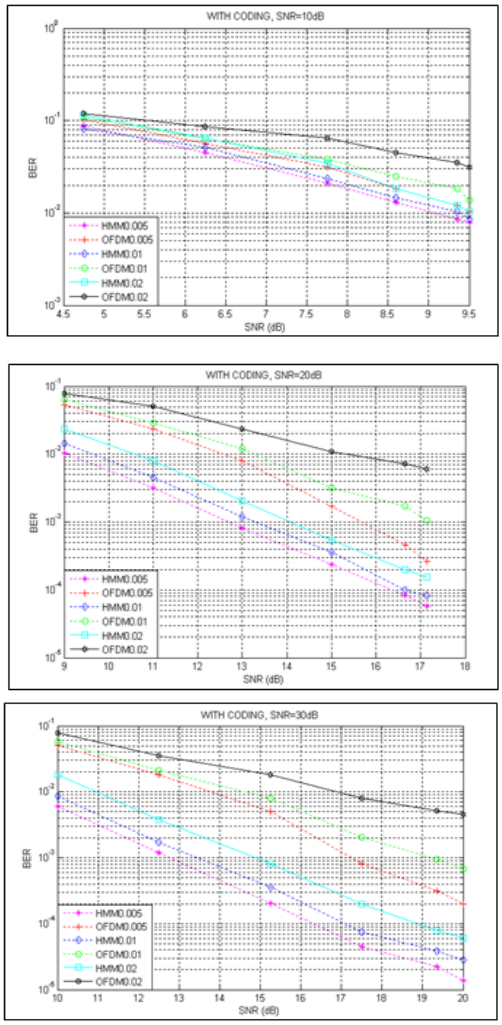

(b)

Fig. 10. Effect of CFO on the BER characteristics of the HMM and OFDM systems (a) without coding (b) with coding.

Table III list the values of BER for different values of TO and CFO, respectively. The results are deduced from Figs. 9 and 10, respectively, for specific values of TO and CFO. Note that HMM system has better BER performance compared with the conventional OFDM system.

To assess the BER enhancement achieved by employing HMM scheme over OFDM scheme we introduce the parameter k_{BER} which is defined as

$$k_{BER} = \frac{(BER)_{OFDM}}{(BER)_{HMM}} \quad (17)$$

where both BERs should be measured at the same operating conditions. In the absence of offset (i.e, $\Delta t=\Delta t=0$), k_{BER} is estimated to be 1.5, 4.6, and 7.2 at SNR=10, 20, and 30dB, respectively, when RS coding is not used. These values are to be compared with 2.2, 23.2, and 56.7 in the presence of coding. These values approximately hold true when $\Delta t=10\%$ at $\Delta f=0$. When $\Delta t=-10\%$, k_{BER} changes to 1.3(1.5), 3.2(10.7), and 3.8 (14.5) in the absence (presence) of coding at SNR=10, 20, and 30dB, respectively. In the other hand, when $|FO|=10\%$ and $\Delta t=0$, k_{BER} reads 1.8(2.9), 6.3(37.0), and 9.8(115.2) in the absence (presence) of coding, respectively. Investigating these results reveals the following findings

- The BER enhancement k_{BER} increases in the presence of coding even with the existence of time offset and carrier frequency offset.
- k_{BER} decreases in the presence of negative timing offset.
- k_{BER} increases in the presence of carrier frequency offset and this effect is more pronounced at the presence of coding.

TABLE II: BER IN THE ABSENCE OF TIME AND CARRIER FREQUENCY OFFSET

SNR (dB)	$\tau_{rms}f_d$	BER			
		Without coding		With coding	
		HMM	OFDM	HMM	OFDM
10	0.005	0.02472	0.0275	0.008576	0.01028
	0.01	0.003309	0.00770	0.0001814	0.000808
	0.02	0.0341	0.0502	0.01452	0.03118
20	0.005	0.002344	0.00417	6.82E-05	0.00024
	0.01	1.48E-03	0.00601	8.18E-06	0.00052
	0.02	0.004358	0.02018	0.0002564	0.005973
30	0.005	0.00112	0.00241	4.09E-06	7.50E-05
	0.01	1.48E-03	6.4E-03	8.18E-06	5.89E-04
	0.02	0.002597	0.0187	9.14E-05	0.005184

TABLE III: EFFECT OF TIME OFFSET ON BER IN THE ABSENCE OF CARRIER FREQUENCY OFFSET.'

TO	SNR (dB)	$\tau_{rms}f_d$	BER			
			Without coding		With coding	
			HMM	OFDM	HMM	OFDM
10%	10	0.005	0.02357	0.05386	0.007925	0.03522
		0.01	1.6E-03	0.02472	2.45E-05	0.008576
		0.02	0.0252	0.0662	0.01195	0.05096
	20	0.005	0.00234	0.00417	6.82E-05	0.00024
		0.01	8.8E-04	0.02252	0.000134	0.007261
		0.02	0.00435	0.02018	0.000256	0.005973
	30	0.005	0.00112	0.00241	4.09E-06	7.50E-05
		0.01	0.00100	0.02018	4.09E-06	0.005973
		0.02	0.00259	0.0187	9.14E-05	0.005184
-10%	10	0.005	0.02979	0.0275	0.012	0.01028
		0.01	0.00627	0.00770	0.000555	0.000808
		0.02	0.04013	0.0502	0.0213	0.03118
	20	0.005	0.00330	0.00417	0.000181	0.00024
		0.01	0.00248	0.00601	8.82E-05	0.00052
		0.02	0.00627	0.02018	0.000555	0.005973
	30	0.005	0.00189	0.00241	4.50E-05	7.50E-05
		0.01	2.4E-03	6.4E-03	7.91E-05	5.89E-04
		0.02	0.00486	0.0187	0.000355	0.005184
20%	10	0.005	0.02472	0.09089	0.008576	0.08741
		0.01	1.8E-03	0.0662	2.45E-05	0.05096
		0.02	0.0275	0.085	0.01028	0.08131
	20	0.005	0.00241	0.06189	7.50E-05	0.04534
		0.01	9.9E-04	0.06189	4.09E-06	0.04534

		0.02	0.00274	0.0662	9.95E-05	0.05096
		0.005	0.00099	0.0502	4.09E-06	0.03118
	30	0.01	1.12E-03	0.04351	4.09E-06	0.02375
		0.02	0.00162	0.0502	2.45E-05	0.03118
		0.005	0.03752	0.0275	0.01826	0.01028
	10	0.01	0.01472	0.00770	0.00320	0.00080
		0.02	0.05386	0.0502	0.03522	0.03118
		0.005	0.00571	0.00417	0.00046	0.00024
	20	0.01	0.00578	0.00601	0.00047	0.00052
-		0.02	0.0107	0.02018	0.00172	0.00597
20%		0.005	0.00355	0.002419	0.00019	7.5E-05
	30	0.01	0.00532	6.46E-03	0.00083	5.8E-04
		0.02	0.00915	0.0187	0.00119	0.00518

IV. Conclusions

The signal-to-interference ratio and BER characteristics of a hexagonal multicarrier modulation system have been investigated in a doubly dispersive wireless channel. Simulation results have been obtained in the presence of timing offset, carrier frequency offset, and channel spread factor. The results indicate clearly that the HMM system offers better BER performance compared with a conventional OFDM system and this result is more pronounced in the presence of CFO. Further, using coding will enhance further the performance of HMM system over OFDM counterpart.

References

[1] M. Krondorf and G. Fettweis, "OFDM link performance analysis under various receiver impairments," Vodafone Chair Mobile Communications Systems, Technische Universit ̈at Dresden, D-01062 Dresden, Germany, September 2007.

[2] C. F. Wu, M. T. Shiue, and C. K. Wang, "Joint carrier synchronization and equalization algorithm for packet-based OFDM systems over the multipath fading channel," *IEEE Transactions on Vehicular Technology*, vol. 59, no. 1, January 2010.

[3] I. Barhumi and M. Moonen, "MLSE and MAP equalization for transmission over doubly selective channels," *IEEE Transactions on Vehicular Technology*, vol. 58, no. 8, pp. 4120–4128, Oct. 2009.

[4] G. Qinghua, L. Ping, and D. Huang, "Low-Complexity iterative channel estimation and detection technique for doubly selective channels," *IEEE Transactions on Wireless Communications*, vol. 8, no. 8, pp. 4340–4349, August 2009.

[5] S. Das and P. Schniter, "Max-SINR ISI/ICI-Shaping multicarrier communication over the doubly dispersive channel," *IEEE Transactions Signal Processing*, vol. 55, no. 12, pp. 5782–5795, Dec. 2007.

[6] G. Matz, D. Schafhuber, K. Grochenig, M Hartmann, and F. Hlawatsch, "Implementation of low-interference wireless multicarrier systems," *IEEE Transactions on Wireless Communications*, vol. 6, no. 5, pp. 1921–1931, May 2007.

[7] T. Strohmer and S. Beaver, "Optimal OFDM design for time-frequency dispersive channels," *IEEE Transactions on Communications*, vol. 51, no. 7, pp. 1111-1122, July 2003.

[8] A. M. Tonello and F. Pecile, "Analytical results about the robustness of FMT modulation with several prototype pulses in time-frequency selective fading channels," *IEEE Transactions on Wireless Communications*, vol. 7, no. 5, pp. 1634–1645, May 2008.

[9] X. Jiadong and T. Strohmer, "Pulse construction in OFDM systems via convex optimization," *IEEE Transactions on Communications*, vol. 56, no. 8, pp. 1225–1230, August 2008.

[10] G. Meng, S. Yue-hong, and Y. Zhi-gang; "Maximum doppler spread estimation by tracking the delay-subspace for LOFDM systems in doubly dispersive fading channels," in *Proc. International Conference on Wireless Communications & Signal Processing*, Nov. 13-15, 2009, pp. 1–5.

[11] F. M. Han and X. D. Zhang, "Hexagonal multicarrier modulation: A robust transmission scheme for time-frequency dispersive channel," *IEEE Transactions on Signal Processing*, vol. 55, no. 5, pp. 1955-1961, 2007.

[12] K. Xu and Y. Shen, "Effects of carrier frequency offset, timing offset, and channel spread factor on the performance of hexagonal multicarrier modulation systems," *EURASIP Journal on Wireless Communications and Networking*, p. 8, 2009.

[13] F. M. Han and X. D. Zhang, "MLSD for hexagonal multicarrier transmission with time-frequency localized pulses," *IEEE Transactions on Vehicular Technology*, vol. 57, no. 3, March 2009.

Dr. Asmaa H. Majeed was born in Baghdad, Iraq, in 1968. She received B.Sc. Degree in Electronic and Communication Engineering from the Department of Electrical Engineering/University of Technology /Baghdad /Iraq, then M.Sc degree in Electronic and Communication Engineering from the Department of Electrical Engineering / Baghdad University/Baghdad /Iraq. Received Ph.D. Degree in Electronic and Communication Engineering from the Department of Electrical Engineering/Busrah University /Busrah /Iraq. She is having around 15 years of Teaching Experience. She is a member of the teaching staff at the Department of Laser and Optoelectronic Engineering/College of Engineering/ Al-Nahrain University/ Iraq. She has published 14 papers in national and international journals/conferences. Her research interests include the design of printed antennas, optical communication, telecommunication engineering.